2022

Performance Modeling Of A Thermoelectric Heat Pump Clothes Dryer With Very High Air Flow

Philip Boudreaux

Viral Patel

Chris Hall

Kyle Gluesenkamp

Steve Karman

See next page for additional authors

Performance Modeling of a Thermoelectric Heat Pump Clothes Dryer with Very High Air Flow

Philip BOUDREAUX[1]*, Viral PATEL[1], Chis HALL[1], Kyle GLUESENKAMP[1], Steve KARMAN[1], Dean ELLIS[1], Anthony GEHL[1]

[1] Building Technologies Research and Integration Center, Oak Ridge National Laboratory
One Bethel Valley Road, P.O. Box 2008, MS-6324, Oak Ridge, TN 37831-6324

* Corresponding Author. Phone: 865-576-7835, Email: boudreauxpr@ornl.gov

ABSTRACT

Previous research has shown that a clothes dryer heated by thermoelectric (Peltier) heat pumps can be up to 85% more efficient than a conventional electric-resistance dryer. A previous thermoelectric prototype used a conventional dryer's air flow of 120 CFM (0.06 m^3/s) and provided about 1300 W of thermoelectric heating capacity with an experimentally measured energy factor of 6.89 lb_c/kWh and 84-minute dry time (compared with ENERGY STAR criteria of >3.93 lb_c/kWh and <80 minutes). In this work, an experimentally validated thermohydraulic model is presented that was used to explore the performance of a very high air flow rate thermoelectric heat pump clothes dryer. Modeled performance shows that an energy factor > 7 lb_c/kWh with a dry time < 80 minutes is achievable with an airflow rate of 240 CFM (0.11 m^3/s) and 600 W of thermoelectric heating capacity.

1. INTRODUCTION

Residential clothes drying consume 657 TBtu annually (US Department of Energy, 2022). Although some energy-efficient dryers are available that use vapor compression cycle heat pumps, they have not had significant market penetration. Higher initial product cost and limited availability could contribute to this slow adoption. Instead, most dryers sold today use electric-resistance heating, which is inefficient and expensive to operate. As an alternative approach, Oak Ridge National Laboratory has been developing a solid-state heat pump dryer that utilizes thermoelectric (TE) modules. Early experimental work yielded a combined energy factor (*CEF*; lb/kWh) of 6.51 lbc/kWh—which is the ratio of the clothes' dry weight to the energy consumed to dry them from 57.5% to 4% moisture content—with a dry time of approximately 160 min when using a TE-to-air heat sink heat exchanger (Patel et al., 2018). Additional work incorporated an intermediate pumped-loop heat exchanger between the TE modules and the air to reduce the high air resistance caused by the heat sinks in the TE-to-air heat exchanger. With the secondary pumped-loop heat exchanger, an energy factor of 6.89 lb_c/kWh was achieved with an 84-min dry time (Patel et al., 2021). The team is currently investigating a lower capacity TE-to-air heat exchanger with a faster air flow rate (i.e., faster than conventional dryers) for more efficient clothes drying. The following describes an experimentally validated performance model that incorporates the lower capacity thermoelectric heat pump (TEHP) and faster air flow rate that will be used to drive the development of this concept.

2. BACKGROUND

The prototype fast-thermoelectric dryer (FastTED) has three key differences over a conventional electric-resistance dryer. First, the stock blower is replaced with one that can provide a higher air flow rate. Second, the electric-resistance heater is replaced with a low-capacity TEHP and a TE-to-air heat exchanger. Third, the duct between the heater and the drum is redesigned to reduce the pressure drop over the dryer's entire air flow path. In this paper, the first two differences are discussed. Figure 1 describes the air flow path of the planned prototype. Air from the dryer cabinet is sucked into the hot side of the TEHP, moved up the duct behind the rear of the drum, and then sucked into the drum. As the air exits the drum, the high-speed blower moves the air through the cold side of the TEHP and then out the back of the cabinet.

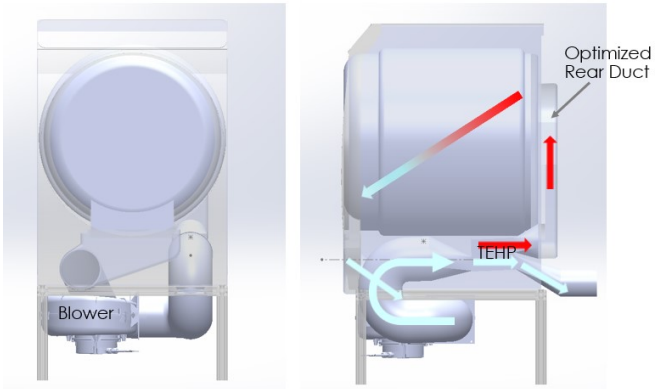

Figure 1: A 3D model of the proposed FastTED prototype

3. MODEL AND ASSOCIATED EXPERIMENTS

The following section describes the model used to predict FastTED performance and the experiments needed to characterize some model inputs—specifically, the hydraulic performance of the high-speed blower connected to the dryer air duct and the thermohydraulic performance of the TEHP.

3.1 Performance Modeling

To model the performance of the FastTED prototype, the Engineering Equation Solver software was used to determine the thermodynamic state of air at the points described in Figure 2. The model calculates the steady-state temperature (T) and humidity (ω) of the air moving through the air path of the dryer (Figure 2).

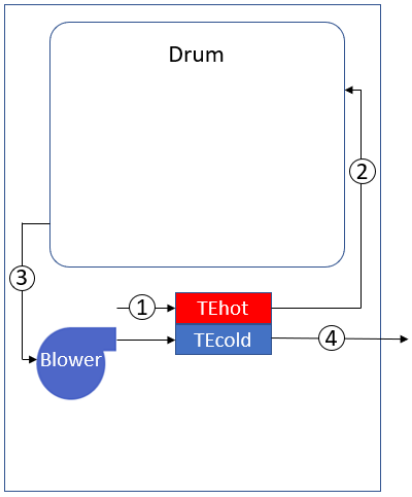

Figure 2: State point diagram for FastTED model

The model assumes a constant mass flow rate ($\dot{m}$) through the air-flow path and therefore does not account for any leakage. It also assumes a constant dryer drum effectiveness for removing moisture from the load. For the

thermodynamic state points, the key equations are listed in Table 1. The ambient air condition is state point 1. State point 2 includes the heat added to the air ($Q_{TE,h}$) from the TEHP. State point 3 describes the air after it interacts with the clothes, and the main difference is an increased humidity ratio (ω) over state point 2. This humidity ratio is described by a global correlation for dryer drum effectiveness (ε) described in earlier work (Gluesenkamp et al., 2019). For details on calculating ω_3, see ω_{out} in Eqs. (1)–(6) from earlier work (Gluesenkamp et al., 2018). State point 4 describes the air after heat ($Q_{TE,c}$) is extracted by the cold side of the TEHP. The air at the dryer exhaust is assumed to be close to saturation at 90% relative humidity (*RH*).

Table 1: Equations for humidity ratio (ω), temperature (T), and enthalpy (H) for each state point of air as it flows through the FastTED

	State point 1	**State point 2**	**State point 3**	**State point 4**
Humidity ratio	ω_1	$\omega_2 = \omega_1$	$\omega_3 = \varepsilon \cdot (\omega_{Surf\ sat} - \omega_2) + \omega_2$	ω_4 (H_4, $RH = 0.9$)
Temperature	T_1	$T_2 = T_1 + Q_{TE,h} / (\dot{m} \cdot C_p)$	T_3 (ω_3, H_3)	T_4 (ω_4, H_4)
Enthalpy	H_1 (ω_1, T_1)	H_2 (ω_2, T_2)	$H_3 = H_2$	$H_4 = H_3 - Q_{TE,c} / (\dot{m} \cdot 1{,}000)$

The dry time (t_{dry}; min) was computed from the difference in humidity ratio between state points 3 and 2, the mass flow rate of the air, and the total amount of water removed from the clothes (m_{water}; kg/s), shown in Eqs. (1) and (2). The total power consumption (W_{total}; W) was calculated, as shown in Eq. (3), using empirically derived equations of blower power as a function of total pressure and TE power as a function of mass flow rate and applied current. The power of the drum rotation motor is constant. The total energy consumed (E; kWh) during the dryer cycle is described by Eq. (4). The *CEF* was computed, as shown in Eq. (5), with the starting moisture content (*SMC*), the final moisture content (*FMC*), the bone-dry weight of the clothes, and the total energy consumed as inputs.

$$\dot{m}_{water} = \dot{m} \cdot (\omega_3 - \omega_2) \tag{1}$$

$$t_{dry} = m_{water} / \dot{m}_{water} / 60 \tag{2}$$

$$W_{total} = W_{TE} + W_{blower} + W_{drum\ motor} \tag{3}$$

$$E = W_{total} \cdot t_{dry} / 60 / 1{,}000 \tag{4}$$

$$CEF = m_{dry\ clothes} / (E \cdot 1.18 \cdot 0.535 / (SMC - FMC)) \tag{5}$$

3.2 Experiments

Two experiments were conducted to enable FastTED performance prediction from the model described above. First, an efficient high-speed blower was installed at the exhaust of the dryer to characterize the blower power consumption and total air-flow-path pressure differential as a function of flow rate. Next, a prototype TEHP with four TE modules and eight extruded plate–fin heat exchangers (one on the cold-side and one on the hot-side of each TE module) was characterized to determine power consumption and heating ($Q_{TE,h}$) and cooling ($Q_{TE,c}$) heat transfer rates as a function of TE current and flow rate.

High-Speed Blower

The original impeller, which was in the air flow path between the filter and the dryer's exhaust, was removed from the arbor of the AC motor in the dryer cabinet. The suction inlet of the new high-flow blower was connected to the exhaust of the dryer. The new blower was operated at different speeds so that the total pressure (measured as the pressure differential between the dryer air inlet and exhaust) as a function of flow rate could be measured (Figure 3). The power consumption as a function of total pressure was also experimentally measured (Figure 4). Figures 3 and 4 also show fit equations that describe the trends, and these equations are used in the model to predict the FastTED performance. For blower performance, given a desired flow rate, the total pressure calculated from the equation in Figure 3 is added to the pressure drop estimated from the TEHP (described in the next section). This

total pressure is then used in the equation shown in Figure 4 to estimate the power consumed by the blower for the desired flow rate.

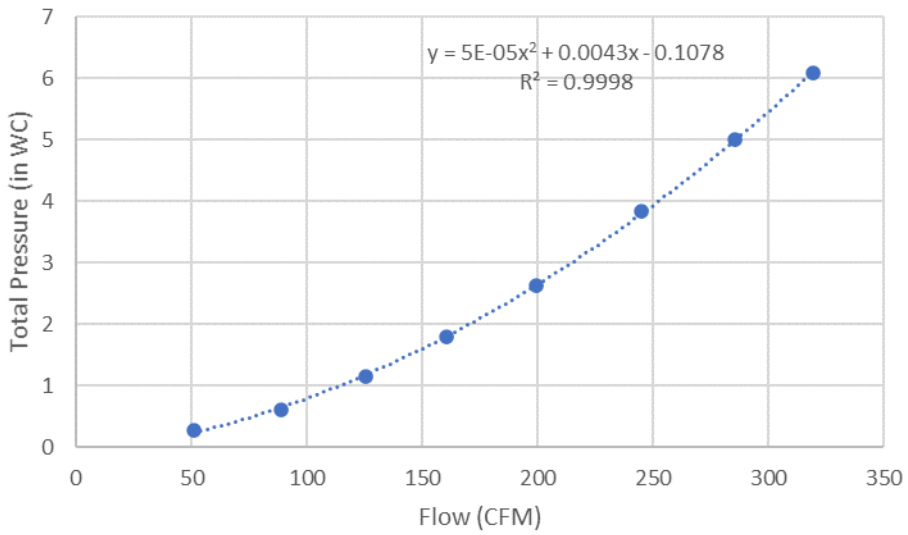

Figure 3: Measured total pressure difference between exhaust and inlet of dryer air flow path as a function of flow rate with high-flow blower installed at exhaust

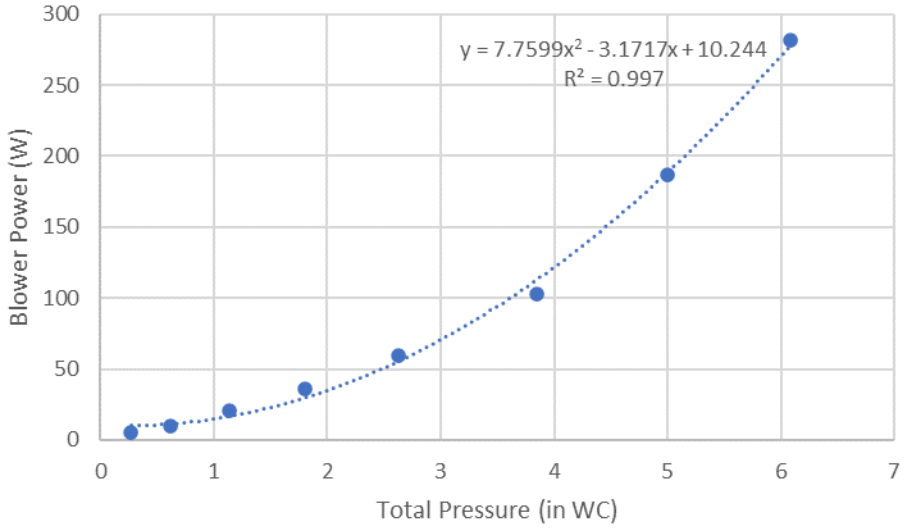

Figure 4: Measured power consumption of high-flow blower as a function of pressure across the blower

TEHP with 4 TEs

A TEHP designed to heat the dryer's inlet air was built and tested using four TE modules connected in series. Each TE module was thermally connected to an extruded plate–fin heat sink to exchange heat generated from the TEs to the air, as shown in Figure 5. Heat is pumped from the air passing through the cold-side heat sinks (blue) to the air passing through the hot-side heat sinks (red). This heat pump was tested at different air-flow rates and TE currents to characterize the pressure resistance, power consumption, and heat extracted from the air on the cold side and the heat added to the air on the hot side. To accomplish this, the differential pressure across the hot (dP_{htaa}) and cold (dP_{ctaa}) sides, the air temperature (T) entering and exiting the cold sides and exiting the hot side, the volumetric air flow rate ($\dot{V}_{htaa}$), and the power consumption of the TEs were measured, as shown in Figure 6.

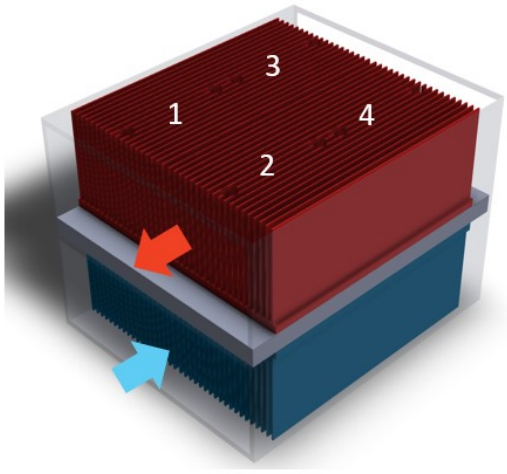

Figure 5: TEHP with four TE generators, each with a cold-side (blue) and hot-side (red) plate–fin heat sink; heat is pumped from the air moving through the cold-side heat sinks (blue arrow) to the air moving through the hot-side heat sinks

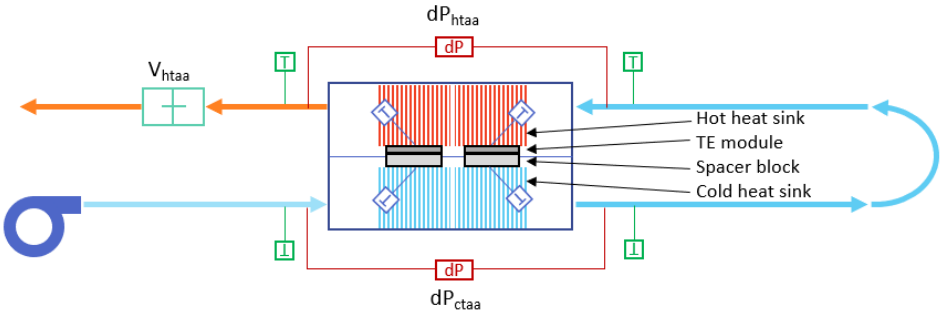

Figure 6: Benchtop test setup for the TEHP with measurements and locations

After completing the experiments, the performance trends ($Q_{TE,h}$, $Q_{TE,c}$, W_{TE}, and dP_{tot}) of the TEHP were described as functions of TE current and/or mass flow rate. Empirically derived formulas for $Q_{TE,h}$ and $Q_{TE,c}$ are shown in Eqs. (6) and (7), where I is the current applied to the four TEs connected in series, and $\dot{m}$ is the mass flow rate of air. These formulas are used for the $Q_{TE,h}$ and $Q_{TE,c}$ model inputs shown in Table 1. The trends are also plotted in Figure 7.

$$Q_{TE,h} = 53.99 \cdot I^{1.37} \tag{6}$$

$$Q_{TE,c} = (339 \cdot \dot{m} + 65.6) \cdot I^{0.4} \tag{7}$$

Equation (8) describes the power consumption of the TEHP as a function of current applied to the TEs and mass flow rate of air. Equation (9) shows the relationship between total pressure ($dP_{tot} = dP_{htaa} + dP_{ctaa}$) across the TEHP as a function of mass flow rate.

$$W_{TE} = (-5.6 \cdot \dot{m} + 6.7) \cdot I^{2.11} \tag{8}$$

$$dP_{tot} = 201.8 \cdot \dot{m}^{1.88} \tag{9}$$

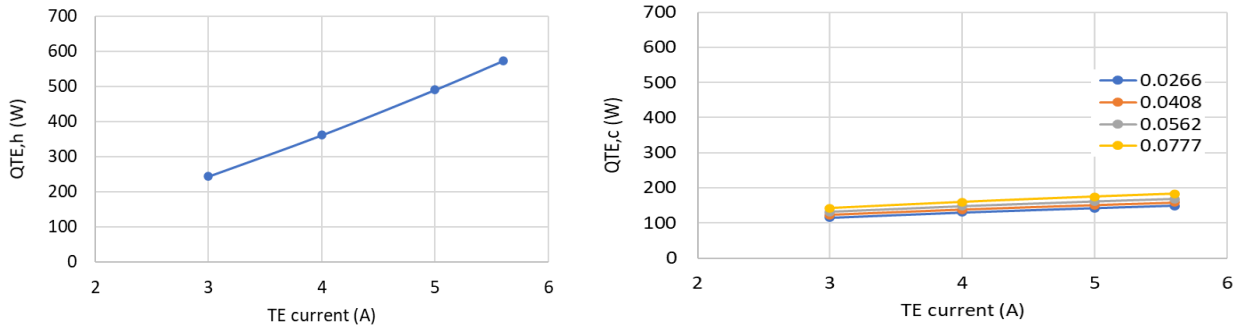

Figure 7: Experimental data with trendlines that describe the heat added to the air on the hot side ($Q_{TE,h}$, left plot) and the heat extracted from the air on the cold side ($Q_{TE,c}$, right plot) of the TEHP as a function of current applied to the TEs and the mass flow rate of air

4. DISCUSSION OF RESULTS

Dryer efficiency tests were completed for no-heat, high-flow rate drying to calibrate and validate the FastTED model. After validation, the model was used to predict the performance of the FastTED under three conditions: no heat drying, TEHP drying, and hybrid drying with both a TEHP and a low-capacity electric-resistance heater. All three conditions were investigated at multiple air-flow rates.

4.1 Model Validation

The model was calibrated by using three standard dryer efficiency tests and the high-speed blower with unheated drying. The tests follow Appendix D1 to Subpart B of Part 430 in the *Code of Federal Regulations*, except the ambient air temperature and RH were not maintained at 75°F ± 3°F (23.9°C ± 1.7°C) and 50% ± 10%, respectively (10 CFR 430, 2017). Table 2 shows the experimental conditions, resulting dry time, and *CEF* for each calibration trial (i.e., C1, C2, and C3). The model was calibrated by developing a trend line of the measured dryer drum effectiveness as a function of volumetric air flow rate ($\dot{V}$) and adjusting a calibration factor (C_f) to match the model-predicted dry times to the experimental dry times of the three trials (see Eq. (9)). The calibrated model was used to predict the performance of another experimental trial that was not in the calibration data set (V1 in Table 2). The model predicted the dry time with a 5% error and the *CEF* with a 6% error. The modeled and experimental *CEF* and dry times are compared graphically in Figure 8.

$$\varepsilon = -0.0016 \cdot \dot{V} + 0.9074 + C_f \tag{9}$$

Table 2: Experimental conditions, dry time, and *CEF* for three experimental trials with unheated drying compared with calibrated model results of the same trials; the last row shows a comparison between experimentally measured performance and the modeled prediction for a dryer test that was not included in the model calibration set

	Experiment					Model	
Trial ID	**T_{in}, °F (°C)**	**RH_{in}, %**	**Flow, CFM (m^3/s)**	**Dry time, min**	***CEF*, lb_c/kWh**	**Dry time, min**	***CEF*, lb_c/kWh**
C1	70.3 (21.3)	48	267 (0.13)	126	9.6	141	8.4
C2	71.1 (21.7)	27	293 (0.14)	95	10.5	98	10.3
C3	72.5 (22.5)	31	259 (0.12)	108	12.0	105	12.7
V1	70.3 (21.3)	47	234 (0.11)	132	10.9	138	10.3

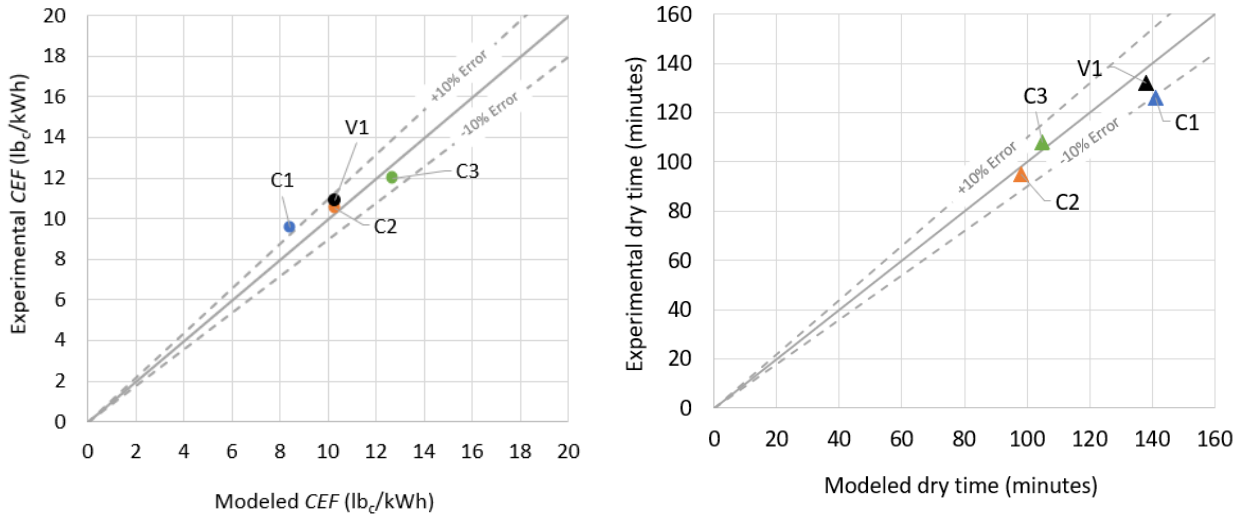

Figure 8: Modeled and experimental *CEF* and dry time compared for 3 calibration test loads and 1 validation test load with high air flow rate and unheated air. The model predicted the *CEF* and dry time of the validation test load within 10% error of the experimental measurement.

4.2 Model Prediction

With the validated model, predictions were made for the performance of the FastTED under three different heating conditions and air-flow rates. First, the performance was predicted for hybrid heating that used the TEHP characterized in Section 3.2 along with a 400 W electric-resistance heater to heat the air. Second, the performance was predicted for TE-only heating with only the TEHP to heat the air. Finally, unheated drying, in which ambient air was used to dry the clothes, was modeled. Each condition was modeled at 10 different air-flow rates that ranged from 100 to 300 CFM (0.05–0.14 m^3/s). Figure 9 shows the model-predicted performance for these three heating conditions at various flow rates. Notably, the performance did not meet the target of *CEF* > 7 and a dry time of less than 80 min. The TEHP increased the total pressure, as described by Eq. (9), and therefore increased the required blower power. This hindered the performance of the air-only drying mode because the TEHP is in the air flow path but is not being used to heat the air.

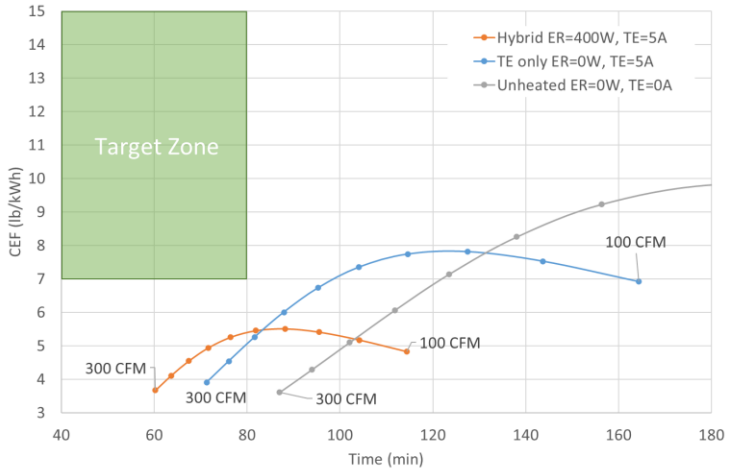

Figure 9: Predicted performance results of FastTED with a high-speed blower and 4× TEHP modifications

To investigate improvements that could be made to a prototype dryer, three changes were made to the model.

1. The original AC motor used to rotate the drum was replaced with a more efficient DC motor, which uses ~33% less power.
2. The total pressure through the air flow path was decreased by 30%; this could be realized by computational fluid dynamics-driven duct geometry optimization.
3. Two additional TE modules were added to the TEHP to increase $Q_{TE,h}$.

After these modifications, the model-predicted performance changed (Figure 10), and the model now shows that operating the FastTED at 240 CFM (0.11 m^3/s) in TE-only mode would enable a *CEF* of over 7 lb_c/kWh with a dry time of less than 80 min. This is indicated by the portion of the blue TE-only curve inside the green box labeled "Target Zone" in Figure 10.

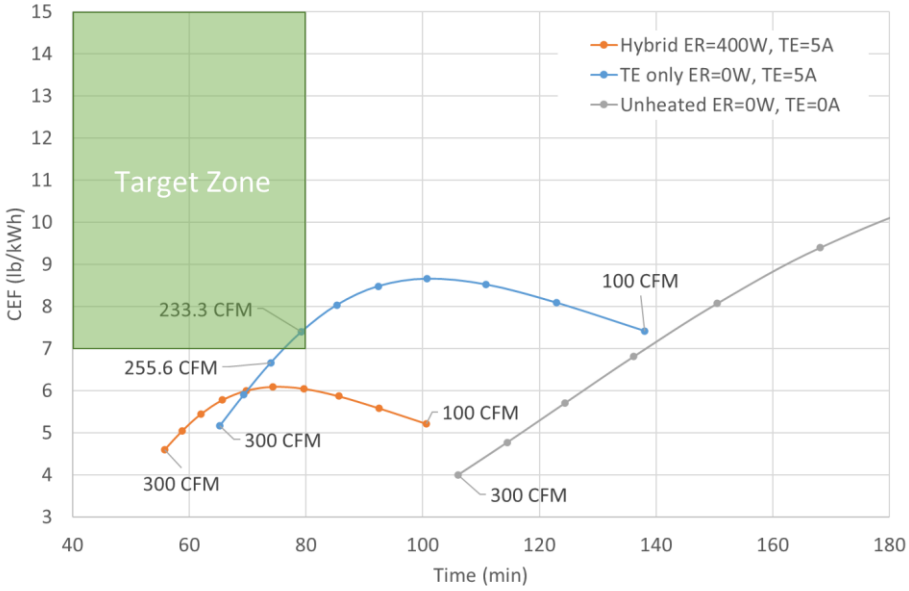

Figure 10: Predicted performance results of FastTED with a high-speed blower, 6× TEHP, reduced pressure along air flow path, and a more efficient drum rotation motor

5. CONCLUSIONS

The authors developed an experimentally validated steady-state thermohydraulic model for hybrid clothes drying using TE modules and electric-resistance elements with high-speed air flow. The model was used to guide residential clothes dryer development and showed that a *CEF* of greater than 7 (lb_c/kWh) and a dry time of less than 80 min is achievable when using a 240 CFM (0.11 m^3/s) flow rate and 600 W of TE heating.

NOMENCLATURE

AC	alternating current
CEF	combined energy factor (lb_c/kWh)
CFM	cubic feet per minute (ft^3/min)
C_p	specific heat (kJ/kg·K)
DC	direct current
dP	differential pressure
E	energy (kWh)
ε	effectiveness (-)
FMC	final moisture content (mass of moisture/mass of bone-dry cloth)
H	specific enthalpy (kJ/kg)
I	current (A)

$\dot{m}$	mass flow rate (kg/s)
m	mass
Q	heat transfer rate (W)
RH	relative humidity
SMC	starting moisture content (mass of moisture/mass of bone-dry cloth)
T	temperature
t	time
TE	thermoelectric
TEHP	thermoelectric heat pump
$\dot{V}$	volumetric flow rate (ft^3/min)
ω	humidity ratio (kg_{water}/kg_{dryair})
W	power (W)
Subscript	
1, 2, 3, 4	state point
c	cold
h	hot
in	entering the drum
out	exiting the drum
$surf,sat$	saturation at the surface
TE	thermoelectric

REFERENCES

10 CFR 430. (2017). *Energy Conservation Program for Consumer Products, Subpart B, Test Procedures; Appendix D1, Uniform Test Method for Measuring the Energy Consumption of Clothes Dryers*. 384–390.

Gluesenkamp, K. R., Boudreaux, P., Patel, V. K., Goodman, D., & Shen, B. (2019). An efficient correlation for heat and mass transfer effectiveness in tumble-type clothes dryer drums. *Energy*, *172*, 1225–1242. https://doi.org/https://doi.org/10.1016/j.energy.2019.01.146

Gluesenkamp, K. R., Boudreaux, P., Shen, B., Goodman, D., & Patel, V. (2018). Experimental Measurements of Clothes Dryer Drum Heat and Mass Transfer Effectiveness. *International High Performance Buildings Conference*, Paper 322.

Patel, V. K., Boudreaux, P. R., & Gluesenkamp, K. R. (2021). Validated model of a thermoelectric heat pump clothes dryer using secondary pumped loops. *Applied Thermal Engineering*, *184*, 116345. https://doi.org/https://doi.org/10.1016/j.applthermaleng.2020.116345

Patel, V. K., Gluesenkamp, K. R., Goodman, D., & Gehl, A. (2018). Experimental evaluation and thermodynamic system modeling of thermoelectric heat pump clothes dryer. *Applied Energy*, *217*, 221–232. https://doi.org/https://doi.org/10.1016/j.apenergy.2018.02.055

US Department of Energy. (2022). *Scout Baseline Energy Calculator*. Office of Energy Efficiency & Renewable Energy.

ACKNOWLEDGMENTS

This work was sponsored by the US Department of Energy's Building Technologies Office under Contract No. DEAC05-00OR22725 with UT-Battelle LLC. The authors would also like to acknowledge Dr. Wyatt Merrill, Technology Manager – Building Electric Appliances, Devices and Systems, US Department of Energy Building Technologies Office.